5754 *Chem. Mater.* **2009,** *21,* 5754–5762
DOI:10.1021/cm901163t

CHEMISTRY OF MATERIALS
Article

Two-Dimensional-Hexagonal Periodic Mesoporous Polymer Resin Thin Films by Soft Templating

Jörg Schuster,[†] Ralf Köhn,[†] Andreas Keilbach,[†] Markus Döblinger,[†] Heinz Amenitsch,[‡] and Thomas Bein*[,†]

[†]*Department of Chemistry and Biochemistry and Center for NanoScience (CeNS), University of Munich, Butenandtstrasse 5-13 (E), 81377 Munich, Germany, and* [‡]*Institute of Biophysics and Nanosystems Research, Austrian Academy of Sciences, Schmiedlstrasse 6, 8042 Graz, Austria*

Received April 27, 2009. Revised Manuscript Received August 16, 2009

Two-dimensional (2D)-hexagonal (plane group, *p6mm*) mesoporous polymer resin thin films were obtained through evaporation-induced organic-organic self-assembly of a preformed oligomeric resol precursor and the triblock copolymer template pluronic P123. The polymer resin films were prepared on silicon wafers by spin-coating a mixture of precursor and surfactant in ethanol. Evaporation-induced self-assembly is followed by the formation of a condensed-wall material through thermopolymerization of the precursor oligomers, resulting in mesostructured phenolic resin films. Subsequent decomposition of the surfactant and partial carbonization were achieved through thermal treatment in an inert atmosphere. The films are crack-free with tunable homogeneous thicknesses and show either a 2D-hexagonal or lamellar mesostructure. An additional, yet unknown, three-dimensional (3D) mesostructure was also found. The mesoporous polymer resin films can serve as precursors for various mesoporous carbon structures.

Introduction

Porous carbon materials are omnipresent and essential for a large number of modern applications. Beneficial properties such as high surface area, large pore volume, chemical inertness, or electrical conductivity make them highly desirable for uses such as electrode materials for batteries, supercapacitors, and fuel cells, as well as applications as sorbents for separation and gas storage or as catalyst supports.

Ordered mesoporous carbons (OMCs)[1−3] could offer advantages for several of these applications, compared to traditional activated carbons, which typically consist of disordered microporous amorphous carbon. Possible disadvantages of activated microporous carbon include limited mass transport in the micropores and low conductivity, because of defects.[1]

One of the first strategies for the synthesis of OMCs was the use of mesoporous silica, acting as a hard template. An early example of periodic mesostructured carbon material was presented by Wu and Bein,[4] by filling the cylindrical mesopores of MCM-41 with polyacrylonitrile via radical polymerization, and subsequently creating conducting carbon nanowires through carbonization of the polymer. OMCs were first reported by Ryoo et al.[5] They used the cubic mesoporous silica MCM-48 as a hard template, sucrose as a carbon precursor, and synthesized the carbon replica CMK-1 through pyrolysis of the included precursor. The silica template could be removed by etching with sodium hydroxide solution. With this hard-templating method, which is also called nanocasting, various carbon mesostructures could be synthesized using silica templates with different symmetries (e.g., CMK-1[3] and SNU-1[6]) as replicas of cubic MCM-48 or CMK-3[7] and CMK-5[8] from hexagonal SBA-15. Further work addressed the electronic and electrochemical properties of these materials[4,6,9] and their surface functionalization.[10−12]

A general drawback of hard-templating methods is the need for an inorganic template, and a process that involves several time-consuming and costly steps for the impregnation of the template, and selective etching of the silica with hydrofluoric acid or a sodium hydroxide solution.

*Author to whom correspondence should be addressed. Fax: +49-89-2180-77622. E-mail: bein@lmu.de.

(1) Liang, C.; Li, Z.; Dai, S. *Angew. Chem., Int. Ed.* **2008**, *47*(20), 3696–3717.
(2) Wan, Y.; Shi, Y.; Zhao, D. *Chem. Mater.* **2008**, *20*(3), 932–945.
(3) Chang, H.; Joo, S. H.; Pak, C. *J. Mater. Chem.* **2007**, *17*(30), 3078–3088.
(4) Wu, C.-G.; Bein, T. *Science* **1994**, *266*(5187), 1013–1015.
(5) Ryoo, R.; Joo, S. H.; Jun, S. *J. Phys. Chem. B* **1999**, *103*(37), 7743–7746.
(6) Lee, J.; Yoon, S.; Hyeon, T.; Oh, S. M.; Kim, K. B. *Chem. Commun.* **1999**, No. 21, 2177–2178.
(7) Jun, S.; Joo, S. H.; Ryoo, R.; Kruk, M.; Jaroniec, M.; Liu, Z.; Ohsuna, T.; Terasaki, O. *J. Am. Chem. Soc.* **2000**, *122*(43), 10712–10713.
(8) Kruk, M.; Jaroniec, M.; Kim, T.-W.; Ryoo, R. *Chem. Mater.* **2003**, *15*(14), 2815–2823.
(9) Xing, W.; Bai, P.; Li, Z. F.; Yu, R. J.; Yan, Z. F.; Lu, G. Q.; Lu, L. M. *Electrochim. Acta* **2006**, *51*(22), 4626–4633.
(10) Li, Z.; Dai, S. *Chem. Mater.* **2005**, *17*(7), 1717–1721.
(11) Bazula, P. A.; Lu, A.-H.; Nitz, J.-J.; Schueth, F. *Microporous Mesoporous Mater.* **2008**, *108*(1−3), 266–275.
(12) Wang, X.; Liu, R.; Waje, M. M.; Chen, Z.; Yan, Y.; Bozhilov, K. N.; Feng, P. *Chem. Mater.* **2007**, *19*(10), 2395–2397.

 Published on Web 11/12/2009 © 2009 American Chemical Society

While many mesoporous carbon materials have been made in bulk, it appears that the preparation of thin films following this strategy is more challenging. A major issue is the weak adhesion of the resulting carbon film after etching of the silica template.[13] In an alternative approach, mesoporous carbon films were prepared via the spin coating of sucrose and silica nanoparticles and the subsequent removal of the silica.[14] However, these films contained a disordered pore system.

In contrast to hard templating methods, soft-templating strategies can directly produce the desired mesoporous carbon precursor structure. According to Liang et al.,[1] soft-templating approaches have four key requirements:

(a) they require a polymerizable precursor system;

(b) they also require a suitable surfactant as a structure-directing agent;

(c) this system and surfactant sustains thermal treatments for curing the carbon yielding precursor, but it decomposes before or during carbonization; and

(d) the precursor system should form a stable polymeric wall material that can retain its mesostructure during template removal.

Given these rather demanding requirements, thus far, it is not surprising that only a few systems have been reported for the synthesis of mesoporous carbon.

The first successful soft-templating approach toward mesoporous carbon was published in 1999 by Moriguchi et al.[15] They synthesized organic mesophases of phenolic resin and cetyl trimethylammonium bromide (CTAB), which acted as a surfactant. However, the mesophases were not stable above 200 °C and, thus, no mesoporous carbon could be obtained. Thurn-Albrecht et al.[16] achieved the assembly of asymmetric large diblock copolymers of polystyrene (PS) and poly(methyl methacrylate) (PMMA) to form hexagonal mesostructured films, whose orientation could even be controlled with electric fields.

Liang et al.[17] achieved the self-assembly of a polystyrene-b-poly(4-vinylpyridine) block-copolymer (PS−P4 VP) and resorcinol and formaldehyde as carbon sources, using a vapor infiltration method. Through a sequence of synthesis steps, they ultimately made mesoporous carbon thin films with hexagonally arranged 33-nm pores that were oriented normal to the surface.

In 2006, Meng et al.[18] introduced another promising soft-templating approach by the self-assembly of a low-molecular-weight resol precursor and triblock copolymer templates with polyethylene and polypropylene blocks of variable lengths. They obtained powders with two-dimensional hexagonal (plane group *p6mm*), three-dimensional (3D) bicontinuous ($Ia\bar{3}d$), body-centered cubic ($Im\bar{3}m$), and lamellar mesostructures. Thus mesoporous carbons with surface areas up to 1490 m^2/g and thermal stability up to 1400 °C were realized.

Recently, two new approaches were published. Dai et al.[19] made OMCs with even higher thermal stability, up to 2600 °C. They accomplished the self-assembly of resorcinol/formaldehyde with block-copolymer templates (e.g., Pluronic F127) under highly acidic conditions. An extremely small shrinkage during this high-temperature treatment is another remarkable property of these OMCs. A single-step procedure for self-assembly in aqueous solution was accomplished by Lu et al.[20]

Despite these great achievements in the soft templating of bulk mesoporous carbon materials, the synthesis of mesoporous carbon thin films is still a significant challenge. So far, only very few successful approaches have been published. The vapor infiltration method was used for the aforementioned resorcinol−formaldehyde−(PS−P4 VP) system,[17] resulting in OMC structures. However, the very large block copolymers used in this study are extremely expensive. Very recently, a similar approach was used for a resorcinol−formaldehyde−F127 system.[21] Different unknown mesostructures were found with electron microscopy. A soft-templating pathway that leads to thin films with face-centered orthorhombic (*Fmmm*) symmetry was reported by Tanaka et al.[13] They used evaporation-induced self-assembly (EISA) during the spin coating of synthesis mixtures with resorcinol, phloroglucinol, and formaldehyde as carbon precursors, and Pluronic F127 as a surfactant template under acidic conditions. The authors report a surface area of 436 m^2/g and a pore volume of 0.39 cm^3/g for a sample carbonized at 400 °C, obtained via nitrogen adsorption of a scratched-off film. Despite these recent achievements, the variety of structures, the thermal stability, and the high surface areas and pore volumes of bulk OMCs have not been matched in thin films yet.

Here, we report the synthesis of highly ordered mesoporous polymer resin thin films with two-dimensional (2D)-hexagonal (plane group *p6mm*) order through evaporation-induced organic−organic self-assembly, using only easily available reagents. These films were pyrolyzed to 400 °C and showed spectroscopic signatures of beginning carbonization at this temperature. The polymer resin films were deposited onto silicon wafers via a spin coating of a presynthesized oligomeric resol precursor and the triblock copolymer template Pluronic P123, followed by thermal treatments in inert atmosphere for thermopolymerization, template removal, and partial carbonization. 2D-hexagonal (*p6mm*), lamellar, and another yet-unknown mesostructure were observed, depending on the template-to-precursor ratio in the synthesis. The films are

(13) Tanaka, S.; Katayama, Y.; Tate, M. P.; Hillhouse, H. W.; Miyake, Y. *J. Mater. Chem.* **2007**, *17*(34), 3639–3645.
(14) Pang, J.; Li, X.; Wang, D.; Wu, Z.; John, V. T.; Yang, Z.; Lu, Y. *Adv. Mater.* **2004**, *16*(11), 884–886.
(15) Moriguchi, I.; Ozono, A.; Mikuriya, K.; Teraoka, Y.; Kagawa, S.; Kodama, M. *Chem. Lett.* **1999**, *11*, 1171–1172.
(16) Thurn-Albrecht, T.; DeRouchey, J.; Russell, T. P.; Jaeger, H. M. *Macromolecules* **2000**, *33*(9), 3250–3253.
(17) Liang, C.; Hong, K.; Guiochon, G. A.; Mays, J. W.; Dai, S. *Angew. Chem., Int. Ed.* **2004**, *43*(43), 5785–5789.
(18) Meng, Y.; Gu, D.; Zhang, F.; Shi, Y.; Cheng, L.; Feng, D.; Wu, Z.; Chen, Z.; Wan, Y.; Stein, A.; Zhao, D. *Chem. Mater.* **2006**, *18*(18), 4447–4464.
(19) Wang, X.; Liang, C.; Dai, S. *Langmuir* **2008**, *24*(14), 7500–7505.
(20) Lu, A.-H.; Spliethoff, B.; Schueth, F. *Chem. Mater.* **2008**, *20*(16), 5314–5319.
(21) Kataoka, S.; Yamamoto, T.; Inagi, Y.; Endo, A.; Nakaiwa, M.; Ohmori, T. *Carbon* **2008**, *46*(10), 1358–1360.

crack-free with tunable homogeneous thicknesses of ~60−200 nm.

Experimental Section

Chemicals. Formalin (37 wt % formaldehyde in water) and the triblock copolymer Pluronic P123 (M_w = 5800, $EO_{20}-PO_{70}-EO_{20}$) were purchased from BASF AG, and phenol was purchased from Merck KGaA. All chemicals were used without further purification. Silicon wafers were donated by Siltronic AG.

Synthesis. *Resol Precursor*. A low-molecular-weight precursor for the organic framework was synthesized in a reaction of phenol and formaldehyde in a base-catalyzed process according to Meng et al.[18] The average molecular weight of the resol precursor is expected to be < 500 g/mol (via gel permeation chromatography (GPC)).[18] For the synthesis, 6.1 g of phenol (0.064 mol) were molten in a flask with 1.3 g of 20 wt % sodium hydroxide solution (0.0065 mol). The mixture was heated to 50 °C and then 10.5 g of formalin (37 wt % formaldehyde in water, 0.1295 mol) were added dropwise. The phenol/formaldehyde/NaOH molar ratio was 1:2:0.1. The clear, lightly yellow colored solution was stirred at 75 °C for 1 h and then cooled to room temperature. The precursor solution was neutralized with 1 M hydrochloric acid and the water was removed by vacuum evaporation below 50 °C. The resulting product was redissolved in ethanol to a total weight of 50 g.

SDA Solution. P123 (1.00 g, 0.17 mmol) was dissolved in 20.0 g (0.45 mol) of ethanol to give a 4.76 wt % solution. For a double concentrated (9.52 wt %) template solution, 1.00 g of P123 (0.17 mmol) were dissolved in 9.5 g of ethanol.

Synthesis of Mesoporous Polymer Resin Films with a 2D-Hexagonal Structure (*p6mm*). 2D-hexagonal films were obtained in the phenol/formaldehyde/NaOH/P123 molar ratio range of 1:2:0.1:(0.0063−0.0095), which is equivalent to weight ratios of the SDA and precursor solution from 1:1 to 1.5:1. In a typical preparation, 1 g of the precursor solution was mixed with 1 g of template solution (phenol/formaldehyde/NaOH/P123 molar ratio = 1:2:0.1:0.0063). After stirring for 10 min, a homogeneous solution was obtained. The mesostructured films were synthesized on polished silicon wafers. The wafers were cut into smaller pieces, washed with ethanol, and cleaned in an oxygen plasma for 1 min. The mixed precursor and SDA solutions were deposited dropwise on the wafers through a syringe filter (CHROMAFIL PET-20/15 MS, pore size = 0.20 μm), and spin-coated at 3000 rpm with an acceleration of 1260 rpm/s. The films were tempered at 100 °C for 24 h. For template removal and partial carbonization, the films were heated in a nitrogen flow with a ramp of 1 °C/min to the final temperature (400 °C) with a dwell time of 3 h at that temperature.

Synthesis of Polymer Films with Lamellar Mesostructure. The synthesis parameters for lamellar films were in the phenol/formaldehyde/NaOH/P123 molar ratio range of 1:2:0.1:(0.0126−0.0189, corresponding to a weight ratio of 2:1 to 3:1). In a typical preparation, 1 g of the precursor solution was mixed with 2.5 g of template solution (1:2:0.1:0.0157).

After the same procedures of solvent evaporation during spin coating and thermal treatment, mesostructured lamellar films were obtained.

Synthesis of Polymer Films with an Unknown 3D Mesostructure. The synthesis parameters for this structure involved a phenol/formaldehyde/NaOH/P123 molar ratio of 1:2:0.1:0.0221 (the latter term corresponds to a weight ratio of 3.5:1). In a typical preparation, 1 g of the precursor solution was mixed with 3.5 g of template solution.

For these films, the same procedures of solvent evaporation during spin coating and thermal treatment were performed.

Variation of Film Thickness. To obtain thinner films, the mixtures of precursor and template were diluted with ethanol by weight. The degree of dilution (D1 to D11) represents the total weight of the diluted solution, compared to that of the parent solution (D1). The solutions were spin-coated and tempered as the other samples described previously. The double concentrated SDA solution was used to get thicker films. These solutions are denoted "Dconc". Even thicker films could be made by casting. For this purpose, the solutions were deposited dropwise onto silicon wafers without spin coating. The resulting films were dried at room temperature.

Nomenclature. The films are denoted S-D-T, where S represents the structure (H = hexagonal, L = lamellar, or U = unknown phase), D represents the degree of dilution, and T represents the carbonization temperature. For example, H-D2-400 °C denotes a film with hexagonal structure and a degree of dilution of D2, that has been pyrolyzed at 400 °C.

Characterization. X-ray diffraction (XRD) of the films measurements were performed on a Scintag Model XDS 2000 in $\theta-\theta$ geometry (Cu Kα; λ = 1.54 Å).

The thicknesses of the films were determined by so-called Kiessig fringes, which result from reflections between the film surface and the interface of film and substrate. In the case of very thin and homogeneous films, several orders of these surface wave reflections can be observed. The reflection angles θ_m and θ_{m+1} of two consecutive fringes are related to the film thickness D by the formula

$$D = \frac{\lambda}{2}\left(\frac{1}{\sin\theta_{m+1} - \sin\theta_m}\right)$$

Grazing-incidence small-angle X-ray scattering (GISAXS) experiments were performed at the beamline BL 5.2 L facility at Synchrotrone Elettra (Trieste, Italy). The wavelength of the incident beam was 0.15498 nm (8 keV), and the sample−detector distance was 1105 mm.

Transmission electron microscopy (TEM) data were obtained on a JEOL Model JEM 2011 microscope at an acceleration voltage of 200 kV. The high-angle annular dark-field scanning-transmission electron microscopy (HAADF-STEM) images were recorded with a TITAN Model 80-300 microscope at an acceleration voltage of 300 kV. Cross sections were prepared by dimple grinding and ion polishing. Raman spectra were recorded on a Jobin Yvon Horiba HR800 UV Raman microscope using a HeNe laser emitting at 632.8 nm. Infrared (IR) spectra were measured in reflection mode with a Bruker Model IFS 66v/s instrument.

Results and Discussion

One of the key parameters for the final structure in the EISA processes is the template/precursor ratio. Here, the ratio is denoted as the weight ratio of the precursor and the template solutions, which can also be translated into the molar ratio of the educts phenol, formaldehyde, and Pluronic P123. Mesostructured films could be obtained in a range of 1:1 to 3.5:1 for the template/precursor ratio.

The XRD patterns of the as-synthesized films H-D1-100 °C, L-D1-100 °C, and U-D1-100 °C are shown in

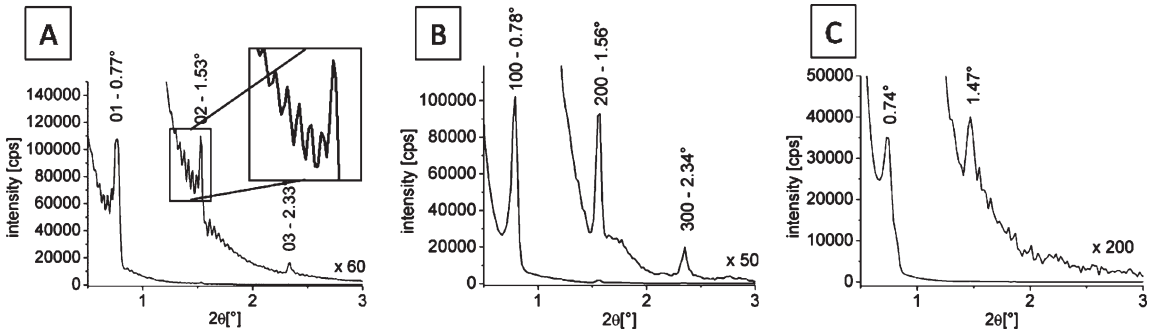

Figure 1. XRD patterns of the as-synthesized samples: (A) H-D1-100 °C, (B) L-D1-100 °C, and (C) U-D1-100 °C. The patterns are magnified in the region of the higher-order reflections, according to the number on top of the magnified graphs. Panel A contains an inset showing Kiessig fringes.

Table 1. Thickness Variation through Dilution of the Synthesis Mixtures

sample name	ratio (template/ precursor)	dilution [wt %]	specific volume (D1 = 1)	thickness (ellipsometry) [nm]
H-Dconc-100 °C	1:1	Conc.	0.738	360
H-D1-100 °C	1:1	0	1	294
H-D2-100 °C	1:1	1	2.05	140
H-D3-100 °C	1:1	2	3.102	73
L-D1-100 °C	2.5:1	0	1	238
L-D2-100 °C	2.5:1	1	2	108
L-D3-100 °C	2.5:1	2	3	67

Figure 1, ordered with respect to increasing template/precursor ratios 1:1, 2:1, and 3.5:1, respectively. Sharp peaks between 0.7° 2θ and 0.8° 2θ can be observed in the patterns with full width at half maximum (FWHM) values between 0.05° 2θ (Figure 1A and 1B) and 0.08° 2θ (Figure 1C). They correspond to well-defined d-values of 11.5−11.9 nm of ordered matter parallel to the substrate. The reflections at higher angles can be indexed as the corresponding higher orders of these first reflections. The intensive and very sharp reflections, in combination with the observation of higher-diffraction orders, confirm the formation of highly ordered mesostructured films. The absence of peaks for further lattice planes reveals the homogeneous orientation of the mesostructures parallel to the substrate plane (with rotational freedom around the substrate normal).

For most of the patterns, Kiessig fringes[22,23] could be observed (e.g., see inset in Figure 1A), which could be used for film thickness calculations.

With ellipsometry, the thicknesses of films with low intensity or without Kiessig fringes could also be measured. The measured values of both methods are in good agreement with each other. Table 1 shows the thicknesses measured with ellipsometry of a dilution series of the hexagonal and lamellar samples (H, L) with template/precursor ratios of 1:1 and 2.5:1, respectively.

The film thickness decreases as the dilution with ethanol increases for both the hexagonal and lamellar films. The lamellar films are slightly thinner, because of the lower concentration of the precursor. The relationship between the thickness and the specific volume is plotted in Figure 2. We define the specific volume as being equal to

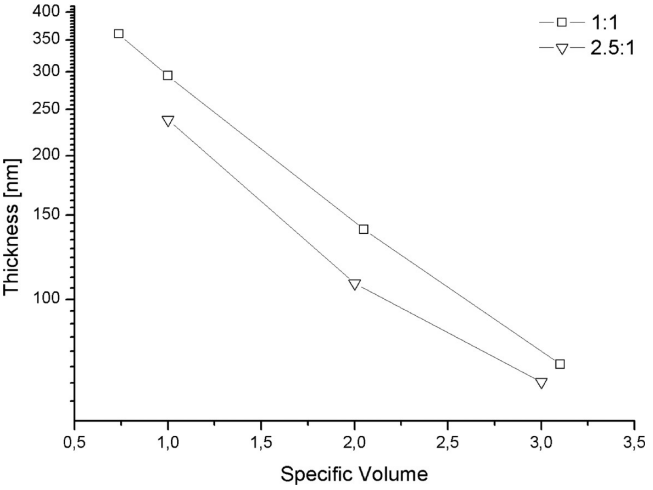

Figure 2. Mesostructured film thickness (logarithmic scale) as a function of the specific volume for (□) hexagonal and (▽) lamellar films.

the volume ratio of ethanol to that of the parent solutions (D1), which can be slightly different from the weight ratios, because of the different densities of ethanol and the parent solutions.

The measured film thickness follows a logarithmic function, with respect to the specific volume in the precursor solution. This allows the prediction of necessary dilution for other desired thicknesses.

2D-Hexagonal Mesostructure (Plane Group *p6mm*). All the films were crack-free and showed homogeneous thickness after pyrolysis at 400 °C. The samples H-D1-400 °C still showed reflections in the diffraction patterns (see Figure 3), while no remaining structure could be observed for the samples L-D1-400 °C and U-D1-400 °C. This already indicates that only a low template/precursor ratio results in a 3D connected wall material. For the higher template/precursor ratios mesostructures without a self-supporting wall material were observed, such as a lamellar or inverse micellar structure.

The measured d_{01}-value of 5.8 nm corresponds to shrinkage of ~50% normal to the surface. Shrinkage during carbonization is a well-known process;[13,18] it occurs because of pyrolysis of the template and condensation reactions in the evolving wall material. For one specific sample (H-D1-100 °C), the overall thickness decreased from 294 nm to 140 nm, which is equivalent to a shrinkage of 52.5%, and a similar 50% shrinkage for

(22) Kiessig, H. *Ann. Phys.* **1931**, *10*, 715–768.
(23) Kiessig, H. *Ann. Phys.* **1931**, *10*, 769–788.

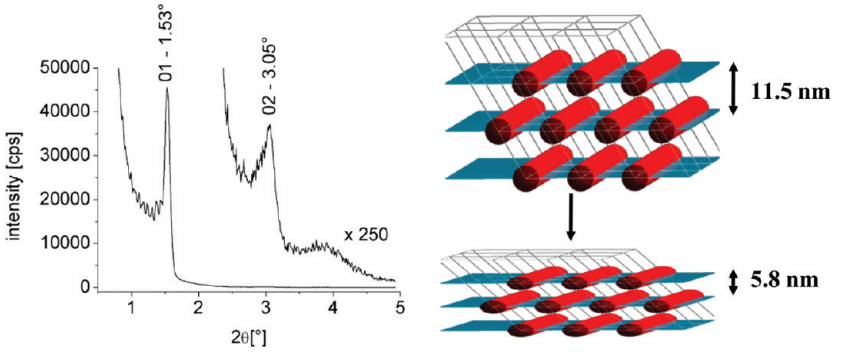

Figure 3. XRD pattern of the sample H-D1-400 °C after pyrolysis. The reflections are shifted to higher angles due to shrinkage. The scheme illustrates the shrinkage during the partial carbonization process.

the lattice plane distances (from 11.5 nm to 5.8 nm) could be extracted from the diffraction data, which can be considered equivalent, considering the measurement accuracy. The films were still crack-free, which shows that the dimensions parallel to the wafer were fixed and shrinkage in these directions did not occur. Therefore, an overall decrease of the film volume can only be caused by thickness shrinkage. For an initial 2D-hexagonal structure with *p6mm* symmetry, the uniaxial shrinkage results in the plane group *c2mm*. In projection along the columns, the pore shape becomes elliptical. Films heated to 600 °C do not show periodic order in XRD measurements, in contrast to the mesoporous carbon powders reported by Meng et al.,[18] which were stable up to 1400 °C. We note that the distortion for thin films can only occur in the direction perpendicular to the substrate; thus, the distortion of the initial unit cell is large and finally results in the collapse of the periodic mesostructure. For powders, the initial unit cell can shrink in all directions, which implies that it does not necessarily have to be distorted.

Synchrotron GISAXS experiments were conducted to identify the highly ordered 2D-hexagonal mesostructure as averaged structural information of the entire film, and to specify the unit-cell parameters in terms of distortion during the thermal treatments. The patterns depicted in Figure 4 for the samples H-cast-100 °C, H-D1-100 °C, and H-D1-400 °C show diffraction spots that can be attributed to a 2D-hexagonal lattice of cylinders, with the cylinders being oriented parallel to the substrate.

All the patterns show very intense reflections, which can be analyzed regarding their *d*-values and φ angles, where φ is defined as the angle between the connection of a peak with the zero beam and the horizontal axis. The peaks at $\varphi = 90°$ come from the lattice planes parallel to the surface, and their positions correspond to the data obtained in the one-dimensional (1D) experiments. Peaks along other directions ($\varphi < 90°$) are related to lattice planes that cut the substrate plane at the angle ($90° - \varphi$). The sample H-cast-100 °C showed the most intense pattern with several higher-order reflections (see Figure 4A). Similar patterns have been reported for 2D-hexagonal silica films.[24,25] All the reflections lie on a reciprocal lattice of a slightly distorted 2D-hexagonal structure and could be indexed according to corresponding lattice planes. For the 2D-hexagonal structure, φ is nominally 30° for the 01 and the $\bar{1}1$ reflection, respectively but strains (e.g., through shrinkage) can change these angles. In Figure 4B, $\varphi \approx 32°$, which is close to ideal, considering the measurement accuracy. In pattern C, for sample H-D1-100 °C, the equivalent reflections could be observed, which reveals the hexagonal structure. This pattern does not show higher orders, because of its lower thickness of ~140 nm. In this pattern, the position of the zero beam cannot be defined very accurately; therefore, the reflections are somewhat shifted and a quantitative evaluation of the *d*-values and angles from Figure 4C was not possible. However, the same structure is expected here, because of coincident *d*-values from the XRD patterns and the similar GISAXS patterns. For the cast film H-cast-100 °C in Figures 4A and 4B, the d_{10}-value (11.6 nm) and φ in combination with the d_{01}-value (11.2 nm) were used to calculate the unit-cell parameters after the thermopolymerization. The results are illustrated in Figure 5. In the same figure, we also show a unit cell, which was modified, in terms of shrinkage by 50%, and exclusively perpendicular to the substrate.

The unit-cell parameter *a* is parallel to the substrate and, therefore, should not be changed by shrinkage. Figure 4D shows the GISAXS pattern after pyrolysis. The decrease of the *d*-values and the increase of φ show the distortion of the unit cell, in agreement with the calculated unit cell in Figure 5.

Figure 6 displays a transmission electron microscopy (TEM) cross section of sample H-D1-400 °C, showing the 2D-hexagonal structure projected along the columns (Figure 6A) and tilted out of the columnar projection (Figure 6B). The images reveal the highly homogeneous mesoporous structure, the constant film thickness, and the elliptically shaped pores.

Figure 6A was recorded along the columns with a small underfocus. At first approximation, the low resolution

(24) Gibaud, A.; Grosso, D.; Smarsly, B.; Baptiste, A.; Bardeau, J. F.; Babonneau, F.; Doshi, D. A.; Chen, Z.; Brinker, C. J.; Sanchez, C. *J. Phys. Chem. B* **2003**, *107*(25), 6114–6118.

(25) Smarsly, B.; Gibaud, A.; Ruland, W.; Sturmayr, D.; Brinker, C. J. *Langmuir* **2005**, *21*(9), 3858–3866.

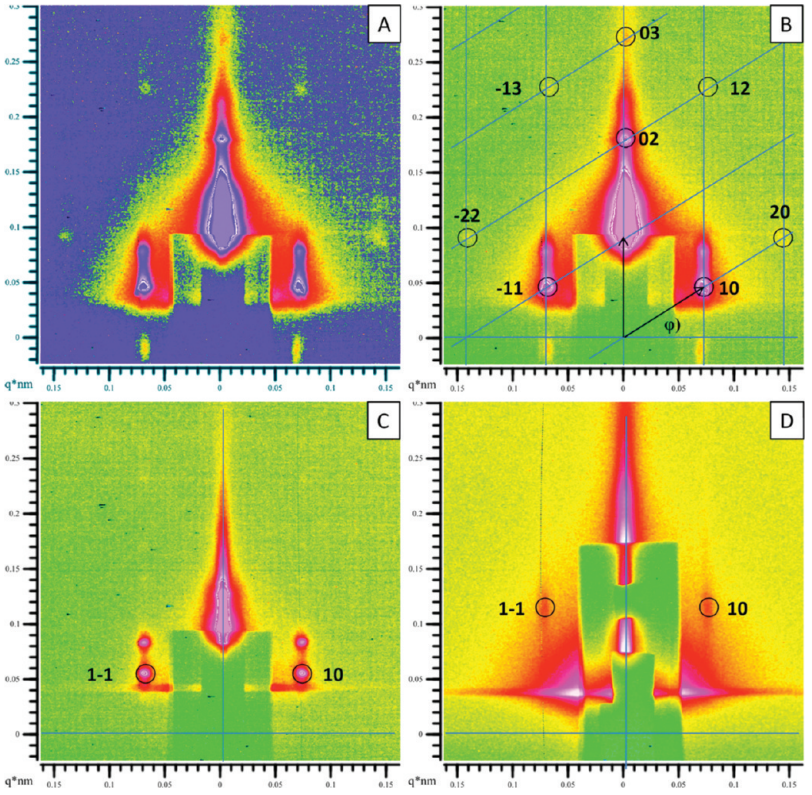

Figure 4. 2D GISAXS patterns: (A) Contrast enhanced image of H-cast-100 °C, where the higher-order reflections can be observed easily; (B) H-cast-100 °C with a linear intensity scaling, visualizing the reciprocal lattice of the 2D-hexagonal structure (the peaks are indexed in a 2D-hexagonal unit cell); (C) H-D1-100 °C before pyrolysis; and (D) H-D1-400 °C after pyrolysis. The indexing according to a 2D-hexagonal unit cell was retained, although it was distorted during template removal and pyrolysis. The most intense reflections in patterns A−C are doubled, because of the grazing incidence geometry; the first peak resulted from the X-rays scattered at the lattice planes, and the second on top is a specular reflection of the first one.

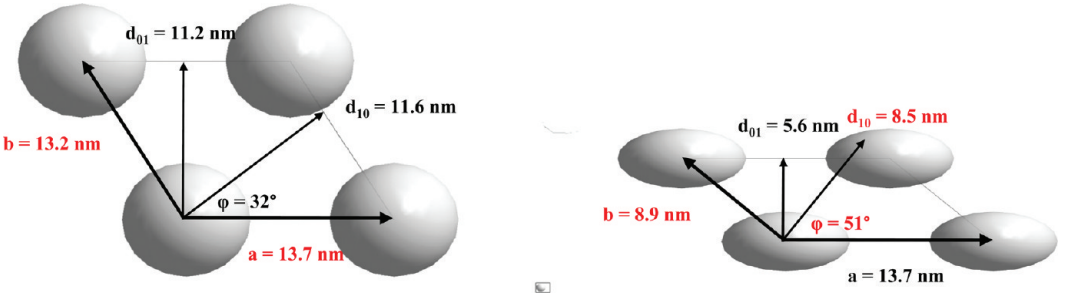

Figure 5. Unit-cell parameters from GISAXS data for the hexagonal cast film before pyrolysis (left) and after pyrolysis (right), applying a shrinkage of d_{01} by 50% and a constant parameter a. The calculated values are given in red.

that is required allows for an interpretation in terms of mass−thickness contrast. The FWHM of the intensity variations perpendicular and parallel to the film surface were used to estimate an average pore size and average cell parameters from more than 20 pores in each case. The values for the minor and major axes, as determined by TEM, were in the range of 3 ± 0.4 nm and 6.8 ± 0.6 nm. These results were confirmed by complementary HAADF-STEM images (see Figure 6C), which allow a direct interpretation in first approximation. The ratio of the minor axis to the major axis is 0.5, which is equivalent with a shrinkage factor of 50%, assuming a perfect hexagonal columnar pore system and disklike cross sections of the pores before pyrolysis and thermopolymerization. This ratio is in good agreement with the shrinkage observed in the XRD measurements and is also in the accuracy range of the pore diameters determined from the TEM image (see Figure 6A).

The unit-cell dimensions extracted from these measurements are displayed in Figure 6D. They are in good agreement with the calculated unit cell from the GISAXS measurements previously shown. The open porosity of the mesoporous films is indicated by large contrast variation (see Figure 6 C). The elliptical shape of the pores is also clearly visible. We note the lower contrast for pores that are near the wafer and, therefore, are far away from the surface of the film. Some of the pores are not completely empty. We suppose that some of the pyrolysis products could not leave the pores during the pyrolysis.

Framework Constitution: 2D-Hexagonal Mesostructure. The constitution of the wall material and the template

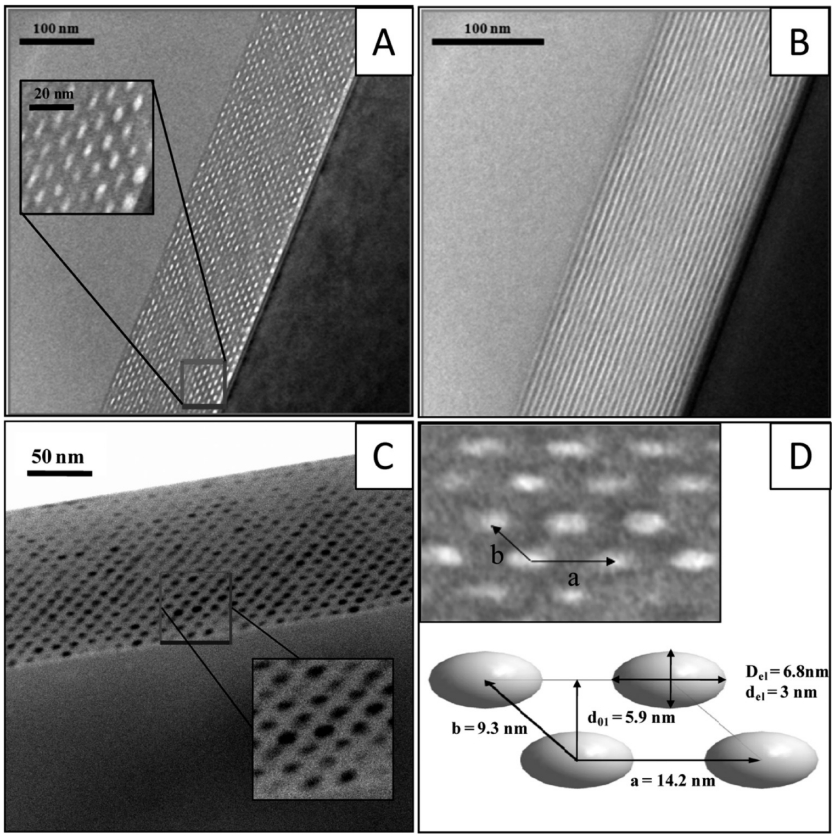

Figure 6. TEM cross section of sample H-D1-400 °C, showing the formerly 2D-hexagonal structure (A) projected along the columns, with an inset at higher magnification, and (B) tilted out of the columnar projection. (C) HAADF-STEM image recorded along the columns; the white area in the image stems from the silicon wafer. (D) Depiction of the base vectors in the TEM micrograph and in the unit cell; the estimated dimensions of the elliptically shaped pores are also depicted.

were investigated using IR spectroscopy. As discussed below, the peaks can be related to the vibrations of functional groups.[18,26] The comparison of films before and after thermal treatment at 400 °C is depicted in Figure 7.

The spectra are comparable to the spectra of polymer resin powders synthesized with the same template/precursor ratio synthesized by Meng et al.[18] The composite of the phenolic resin and the template shows several peaks related to vibrations of substituted benzene rings:[26] The broad band at ~3300 cm^{-1} arises from the O−H stretching of phenolic or aliphatic hydroxyl groups. The peaks observed at ~3000 cm^{-1} can be related to the aromatic and aliphatic C−H stretching. The peak observed at 1611 cm^{-1} is caused by C−C bond stretching of trisubstituted benzene rings. The band near 1475 cm^{-1} is caused by C−H bending of an aliphatic bridge structure. The intense band at 1130 cm^{-1} can be related to C−O stretching in the template. All the bands nearly vanished after the heat treatment, especially the bands for aliphatic C−H stretching and the C−O stretching modes in the template, which confirms the decomposition and removal of the surfactant template. Only one band at 1254 cm^{-1} remains or is even increasing in intensity for all samples heated to 400 °C. According to Trick et al.,[26] it is related to diphenyl ether bridges, which are formed at temperatures of ~400 °C, giving evidence of the increasing degree of crosslinking.

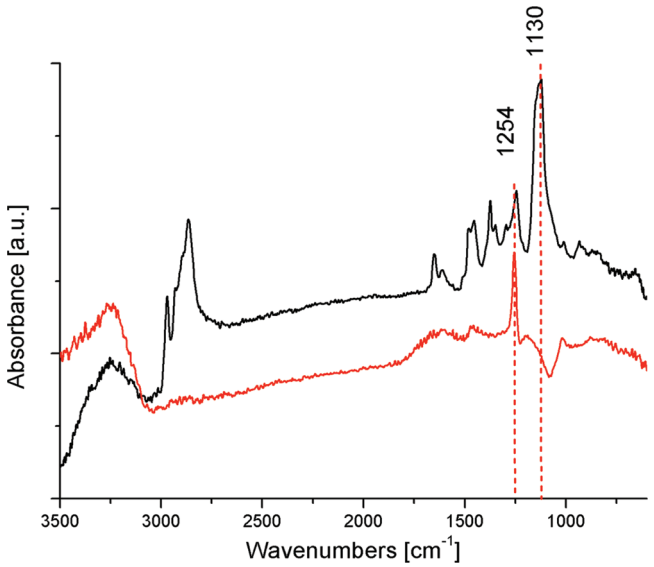

Figure 7. IR spectra of an as-synthesized thin film (H-D1-100 °C) (black trace), and after template removal and pyrolysis at 400 °C (red trace) (H-D1-400 °C). The peak related to the template at 1130 cm^{-1} vanished because of pyrolysis of the template.

Figure 8 shows two films on glass slides: a colorless one before pyrolysis and a brown one after pyrolysis.

(26) Trick, K. A.; Saliba, T. E. *Carbon* **1995**, *33*(11), 1509–1515.

The absorption of light in a broad energy range is caused by the evolving amorphous carbon that contains small graphitic domains. Even after pyrolysis, the films remain transparent, which we attribute to their small thickness of only 140 nm, whereas powders are already deep black after pyrolysis at 400 °C. Raman spectroscopy has been proven to be useful for the investigation of the microstructure of amorphous or graphitic carbon materials.[27] A Raman spectrum of a pyrolyzed film is shown in Figure 9.

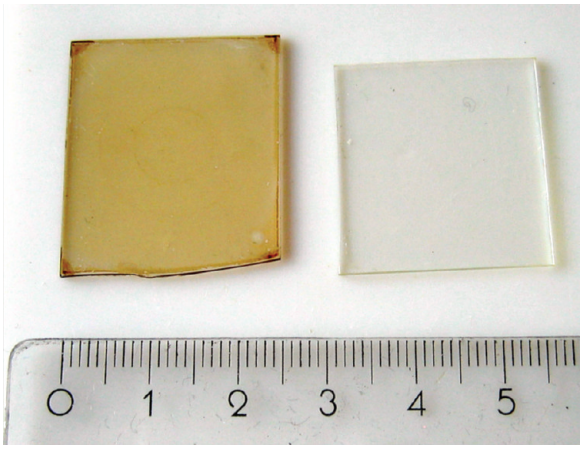

Figure 8. Films on glass slides as-synthesized H-D1-100 °C (right) and H-D1-400 °C after pyrolysis at 400 °C (left).

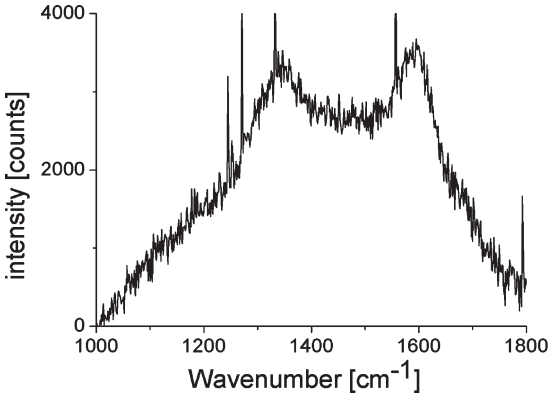

Figure 9. Raman spectrum of the sample H-D1-400 °C, pyrolyzed at 400 °C, showing the broad carbon D and G bands at 1358 cm^{-1} and 1600 cm^{-1}; the spikes are detector artifacts.

The well-known broad D and G bands of partially graphitic carbon are visible at 1358 cm^{-1} and 1600 cm^{-1}, respectively. The D band is a breathing mode of six-carbon aromatic rings, which is forbidden in perfect graphene sheets and, thus, it is associated with small domain sizes. The G-band is a vibrational mode of in-plane bond stretching of pairs of sp^2 C atoms, which is symmetry-allowed in ideal graphene sheets. The presence of the two bands at almost equal intensity is typical for nanocrystalline graphitic carbon generated by pyrolysis of organic precursor materials.[13,18]

Lamellar Phase and an Unknown Mesostructure. GISAXS patterns for the samples L-D1-100 °C and U-D1-100 °C are presented in Figure 10.

Only peaks on the vertical axis ($\varphi = 90°$) are visible in Figure 10A, which proves the lamellar structure of the film. Lamellar structures are commonly formed for the highest template/precursor ratios with Pluronic P123 as a template.[18] Thus, it is surprising that, for a sample with an even higher template/precursor ratio (U-D1-100 °C), further reflections became visible. Because the structure was not stable upon template removal, and the ratio was higher than for the lamellar structure, we tentatively propose the formation of an inverse micellar structure in this sample. For example, possible structures include a reverse micellar arrangement of 3D ordered spheres of the carbon precursor surrounded by the template, or a hexagonal arrangement of carbon cylinders surrounded by the template, respectively. The GISAXS peak positions of this sample are similar to the pattern of the 2D-hexagonal structure, suggesting the formation of an inverse micellar structure with *p6mm* symmetry.

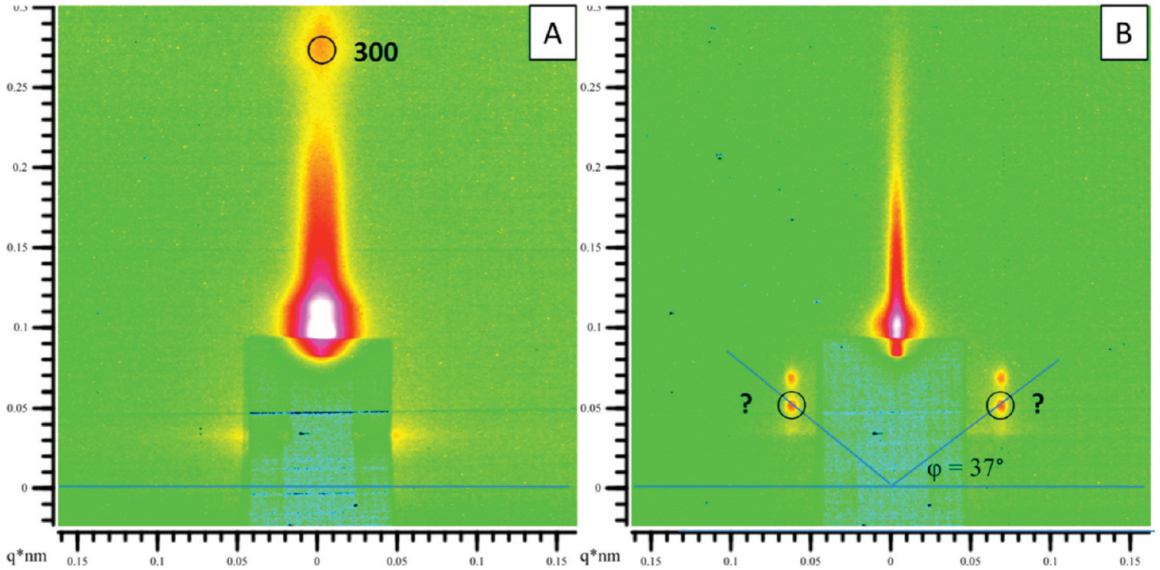

Figure 10. GISAXS patterns of (A) a lamellar structured film (L-D1-100 °C) and (B) a film for higher template concentration with unknown mesostructure (U-D1-100 °C).

Conclusions

In this work, we have demonstrated the synthesis of highly ordered mesoporous polymer resin thin films through the partial carbonization of organic−organic composite films. Using a soft-templating method, thin films with several mesostructures were formed during the evaporation-induced self-assembly of a preformed precursor and a block-copolymer template at variable molar ratios. The template removal upon pyrolysis from films with low template/precursor ratios leads to a compressed but still highly ordered mesostructure. The structural distortion during pyrolysis (from plane group *p6mm* to *c2mm*) through uniaxial shrinkage along the substrate normal was followed with grazing-incidence small-angle X-ray scattering (GISAXS) measurements for the 2D-hexagonal phase. The structural parameters and the porosity could be directly visualized using transmission electron microscopy (TEM) and high-angle annular dark-field scanning-transmission electron microscopy (HAADF-STEM) images of cross sections in columnar projection. This soft-templating approach represents a simple and inexpensive source for mesoporous polymer resin and carbon films, which can serve as a structural platform for various applications that require highly stable mesoporous channel structures.

Acknowledgment. The authors thank the NIM cluster, CeNS, and the DFG (SFB 486) for their support of this work. Beam time at the synchrotron Elettra (Trieste, Italy) is gratefully acknowledged.

Supporting Information Available: X-ray diffraction pattern for the film H-cast-100 °C. (PDF) This material is available free of charge via the Internet at http://pubs.acs.org.

(27) Ferrari, A. C.; Robertson, J. *Phys. Rev. B* **2000**, *61*(20), 14095–14107.